Polyhedron 103 (2016) 141–149

Contents lists available at ScienceDirect

Polyhedron

journal homepage: www.elsevier.com/locate/poly

Revisiting $Ir(CO)_3Cl$

Yuta Tsuji [a], Roald Hoffmann [a,*], Joel S. Miller [b]

[a] Department of Chemistry and Chemical Biology, Cornell University, Ithaca, NY 14853, United States
[b] Department of Chemistry, University of Utah, Salt Lake City, UT 84112, United States

ARTICLE INFO

Article history:
Received 10 August 2015
Accepted 18 September 2015
Available online 3 October 2015

Dedicated in friendship to Malcolm Chisholm, who also likes metal chains

Keywords:
Metal atom chains
Ir compounds
Molecular orbital theory
Metallicity
Oxidation states

ABSTRACT

We return to an old puzzle – the short metal–metal separation and electrical conductivity of the apparently unoxidized one-dimensionally stacked structure of a d^8 Ir(I) complex, $Ir(CO)_3Cl$. One would expect neither a short Ir–Ir distance of 2.84 Å, nor metallicity in an unoxidized stacked square-planar d^8 array. We build up dimer, trimer, one-dimensional polymer and model 3-dimensional structures, in both molecular and extended structure plane wave calculations. The short Ir–Ir separation in the polymer, with a substantial contribution of $6p_z$—$5d_{z^2}$ bonding to it, is obtained without any oxidation. There is computational evidence for an important level crossing in the polymer. The metallicity remains unexplained, but likely arises from partial oxidation. And that remains an outstanding experimental issue.

1. Introduction

From its synthesis and characterization by some of the pioneers of organometallic chemistry, Walter Hieber [1], Ernst Otto Fisher [2], Lamberto Malatesta [3] and their coworkers, $Ir(CO)_3Cl$ has generated more questions than answers. For starters, is the material ever stoichiometric? Compositions such as $Ir(CO)_{2.93}Cl_{1.07}$ [4] and $Ir(CO)_3Cl_{1.1}$ [5] have been suggested, as well the incorporation of $Ir(CO)_2Cl_2$ or chloride into the structure. What appears to be the most definitive structural study, by Reis and Peterson [6,7], was of a sublimed material (copper-brown orthorhombic crystals). The structure is shown in Fig. 1. It contains nearly linear chains of $Ir(CO)_3Cl$ with a relatively short Ir–Ir distance of 2.844 Å. There is no room in the structure for chloride ions (and sublimation would argue against an ionic material). The structure is not without complications, for there is positional disorder between Cl and CO ligands along the chain. This disorder was resolved, in a good refinement [7]. However, while Reis and Peterson are pretty definite about excluding any $Ir(CO)_2Cl_2$ units in the chains, revisiting the structure with updated disorder algorithms may provide further insight with respect to disorder.

Why worry about the dichloride or excess halide? Because

(a) The Ir–Ir distance is relatively short, and such diminution of metal–metal separations is indicative of metal oxidation away from the d^8 electron count, as occurs in the platinum blues, and in many related compounds [9]. There are square planar d^8 complexes of Ir(I) (with a ligand set different from $Ir(CO)_3Cl$) that form stacks, but they have substantially longer Ir–Ir distances, 3.2 Å or greater [10–14]. One example is shown in Fig. 2a [12].
(b) One has a variety of Ir compounds with d-electron counts between 7 and 8, i.e., oxidation states of Ir between +2 and +1. Some form extended chains, some are capped oligomers. Older compounds in this series include $A_{0.60}Ir(CO)_2X_2$, with A = K, Cs, TTF (TTF = tetrathiafulvalene) [15]. Newer ones arise from electrochemically oxidized $[Ir(CO)_2X_2]^-$, X = Cl, Br, I [16,17]. And there is the beautiful series of partially supported oxidized Ir chains from the Oro and Ciriano groups [18–22], one example of which is shown in Fig. 2b, [20]. The Ir–Ir distances in these compounds decrease with increasing oxidation, and are in the range of 2.70–2.80 Å.
(c) A few dimeric (and capped) unsupported Ir(II) complexes are known [23,24]. The Ir–Ir bond length in these is 2.66–2.71 Å. One example is shown in Fig. 2c, [23].
(d) d^8 $[Ir(CO)_2X_2]^-$ anions, X = Cl, Br, exist. There is no stacking in the PPN^+ (PPN^+ = bis(triphenylphosphane)iminium cation) salt structure [25], but there is experimental and theoretical evidence for one-dimensional chains with Ir–Ir 2.82 Å in the K^+ salt [26].
(e) There have been persistent reports of the weak metallicity of $Ir(CO)_3Cl$. The measurements were made on a material that was reported as nonstoichiometric, $Ir(CO)_{2.90}Cl_{1.10}$, single crystal. The measured room-temperature conductivity in

* Corresponding author.

http://dx.doi.org/10.1016/j.poly.2015.09.050
0277-5387/

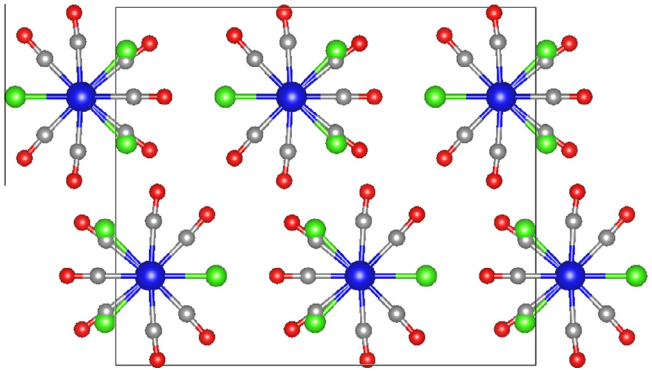

Fig. 1. The crystal structure of $Ir(CO)_3Cl$ constructed from the atomic coordinates reported in the literature [8]; the view is along the chain. Note the excellent packing.

both studies was $0.2\ \Omega^{-1}\,cm^{-1}$ [27,28]. A smaller conductivity was measured for $Ir(CO)_3Br$ [29]. On the face of it, square-planar d^8 is a closed shell electron count; a weakly interacting array of such units should not be metallic unless the Ir is partially oxidized.

A good general summary of the early work on Ir(I) and oxidized stacks may be found in the review by Reis [8]. We decided to reinvestigate the electronic structure of $Ir(CO)_3Cl$; a previous calculation by Bhaumik and Mark exists [30], and one by Ginsberg has been cited in the literature [31]. As will be seen, our study, which we believe is informative in a number of ways, does not resolve the mystery that only future experimental studies will clarify.

2. Results and discussion

2.1. The monomer, dimer, and trimer

In our work, we used a variety of theoretical methods. The details are given in the theoretical methods section at the end of this paper, but they include molecular DFT methods (Gaussian), plane wave extended structure computations (VASP), and extended Hückel calculations. Fig. 3 shows the calculated geometry-optimized structures of the monomer, from a Gaussian molecular calculation (a), a VASP simulation of the monomer (b), VASP is an inherently three-dimensional program; the monomer is simulated by putting it in a cubic lattice, 15 Å away from its replicas), (c) periodic VASP calculation of the one-dimensional polymer (center), and, for comparison, (d) the monomer from the crystal structure of the polymer. The three theoretical structures, one in principle for a gas phase molecule at $T = 0$ K, the other two from plane-wave calculations of a simulated monomer and monomer unit in a polymer, agree pretty well with each other, and match well the observed monomer unit of the crystal structure with respect to distances and even the slight nonlinearity of the *trans*-OCIrCO atoms. The latter is curious, as there should be any steric demands in the molecule.

Fig. 4 shows the energy levels and a selection of the wave functions. While the level scheme of any real molecule is not as simple as that of a textbook d^8 complex, $Ir(CO)_3Cl$ comes close. Note the HOMO, the $5d_{z^2}$ top level of the 4-orbital occupied d-block, some other high-lying levels which are mainly Cl 3p orbitals antibonding to metal d_{xy} and d_{xz}, and the lower-lying unfilled orbitals, clearly carbonyl π^* levels. The gap between filled and unfilled orbitals is large, as expected.

We next optimized gas-phase dimer arrays $[Ir(CO)_3Cl]_2$, and these went into a staggered conformation, as shown in Fig. 5. In carrying out these calculations we had the option of using a functional empirically adjusted for dispersion forces; without including these, the Ir–Ir separation was 3.21 Å, with the dispersion correction, it was 3.05 Å (Gaussian, VASP values were similar). An eclipsed dimer, around 9 kcal/mol higher in energy, was not a local minimum in our calculations.

We also calculated a simulated dimer with plane-wave methods (VASP), as before isolating it from other molecules. The structure is shown in the Supplementary Information (SI); it is similar in detail to that in Fig. 5, distances varying by less than 2%. The optimized Ir–Ir separation in that VASP-computed dimer is 2.98 Å, 0.07 Å shorter than in the Gaussian-calculated dimer. There are unavoidable differences in the calculations; VASP uses a PBE functional, plane wave basis set, and D2 dispersion correction while GAUSSIAN uses the B3LYP functional, localized basis set, and D3 dispersion correction.

Fig. 6 shows the optimized geometries of trimers calculated with VASP and GAUSSIAN. The structures are nearly identical; the Ir–Ir contact a little shorter in the plane-wave computation.

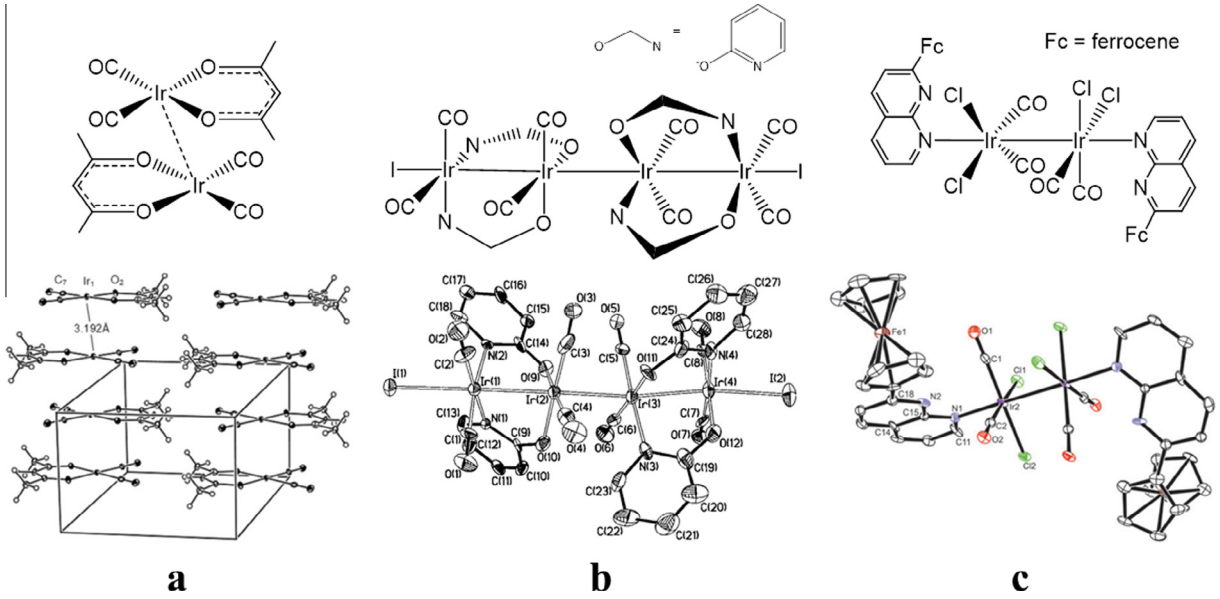

Fig. 2. Examples of other dimeric and oligomeric structures containing stacked Ir dimers or chains in oxidation state (a) +1 [12], (b) +1.5 [20], (c) +2 [23].

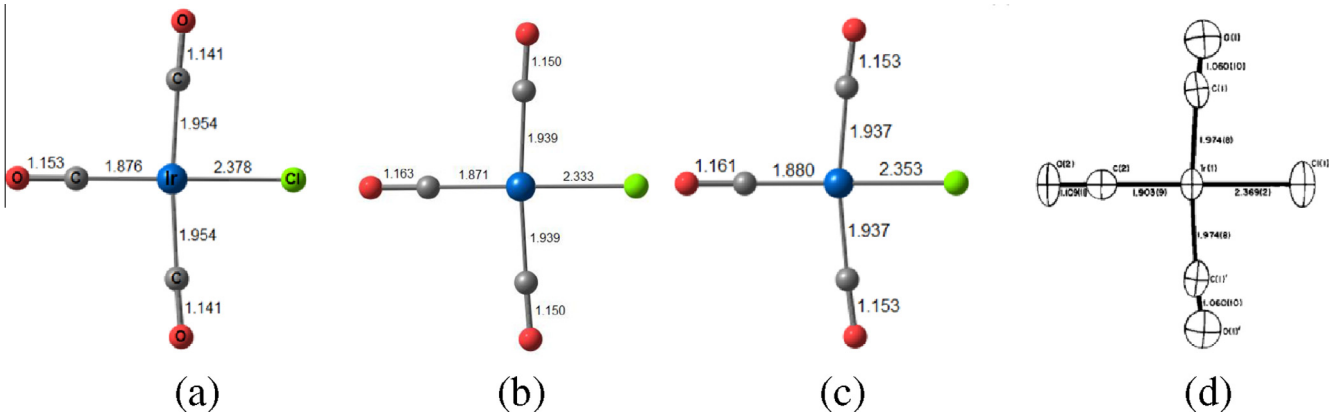

Fig. 3. $Ir(CO)_3Cl$ structures (a) Gaussian-optimized structure of monomer in gas phase, (b) VASP optimized structure of monomer (in a large unit cell, 15 Å from its replicas), (c) VASP-optimized structure, in model of one-dimensional polymer, and (d) experimental structure of monomer unit of polymer in crystal. Throughout this paper, the color code in the models is Ir = blue, C = grey, O = red, Cl = green. (Color online.)

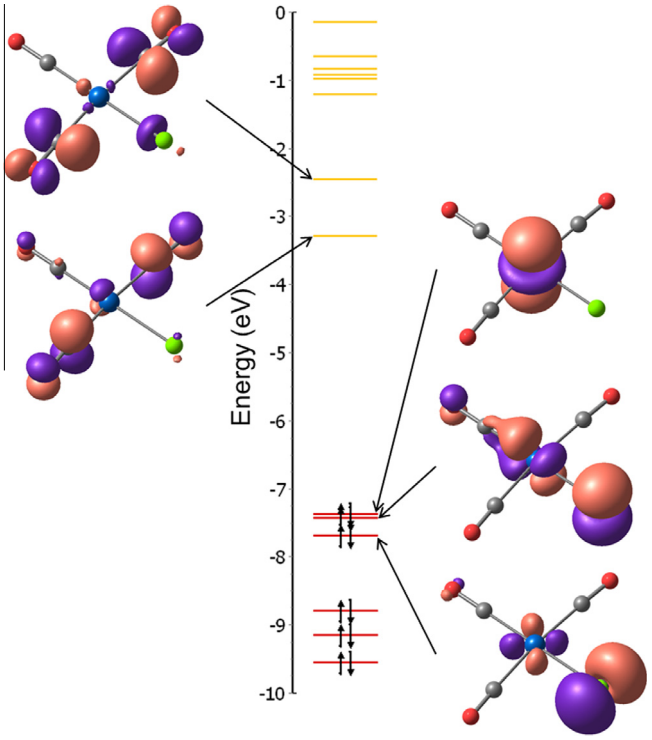

Fig. 4. Energy levels and selected molecular orbitals of $Ir(CO)_3Cl$.

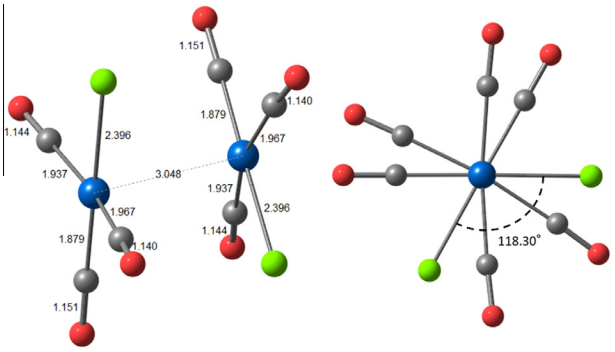

Fig. 5. Calculated optimized geometry for a gas phase dimer of $Ir(CO)_3Cl$.

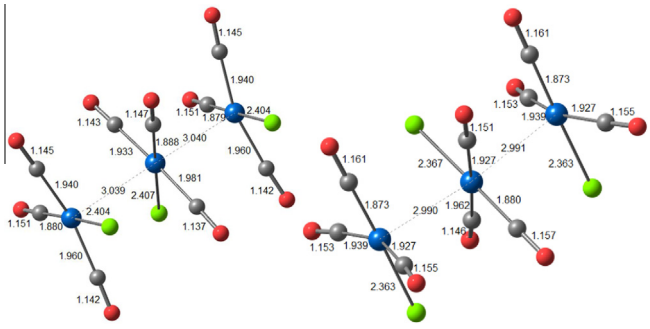

Fig. 6. Optimized trimer geometries, from Gaussian (left), from VASP (right).

2.2. Energetics of oligomerization and the reasons for it

Note the calculated Ir–Ir distance in the dimer is 3.05 Å, 7% longer than in the observed polymer structure in the solid state. Nevertheless, there is moderate interaction between the monomer units. One way this shows up directly is in the energy of dimerization – the dimer is calculated to be more stable than the monomers by 15 kcal/mol. The binding energies calculated by the GAUSSIAN program were corrected using the basis set superposition error (BSSE) counterpoise procedure. The VASP calculation gives the same number. We also calculated the energy of a trimer (see SI), and this was 14 kcal/mol lower in energy than a dimer plus monomer. Or to put it in another way, the energy of oligomerization is 7.5 kcal/mol of monomer in the dimer, and 9.7 kcal/mol of monomer in the trimer. Similar numbers are obtained from VASP calculations.

While the above energies indicate that there is stabilization in aggregation, the Ir–Ir distance does not show much sign of it, as the Ir–Ir decreases by only 0.01 Å going from the dimer to the trimer. In the dimers and trimers of the related $[Rh(alkylisocyanide)_4]^+$ there is a different outcome, as far as distances are concerned [32].

There is good evidence for aggregation of d^8 dimers in solution [33,34], so the general effect – a substantial driving force for aggregation – was anticipated. But the magnitude of the energetics involved came as a bit of a surprise to us.

Novoa, Aullón, Alemany, Alvarez, and their co-workers [35] carried out theoretical studies on the metal–metal interactions in various dimers of d^8-square-planar Pt(II) and Rh(I) complexes at the Hartree–Fock (HF) and second-order Møller–Plesset perturbation theory (MP2) levels. Their studies gave binding energies in the range from 2 to 20 kcal/mol. They also specifically calculated $Rh(CO)_3Cl$ and obtained a dimer binding energy of 3 kcal/mol, at a rather long Rh–Rh separation of 3.55 Å. Zhou et al. [36] calculated

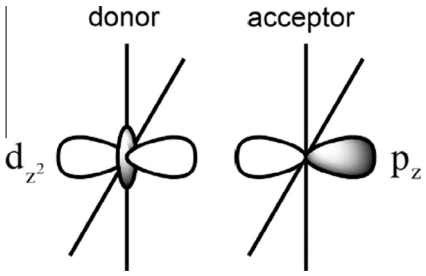

Fig. 7. Schematic representation of the orbital interaction between d_{z^2} and p_z orbitals of two units in an aggregate.

a dimerization energy of 8 kcal/mol for the dimer of another Pt(II) complex. Xia et al. [37], studying experimentally and theoretically a Pd(II) dimer, calculate a dimerization energy of around 16 kcal/mol, of which the contribution from the metal–metal bonding interaction is around 8 kcal/mol. Poater et al. [38] theoretically and experimentally examined a trimeric Pt(II) complex, and reported that the energy of the trimer is about 9 kcal/mol lower than a dimer plus monomer, but additional interactions between ligands, such as π–π stacking and hydrogen bonds, increase the binding energy to about 44 kcal/mol. In general these studies give dimerization energies similar to what we obtain.

In the energy level diagram for the dimer (see SI) there is also indication of some interaction between the monomers, but the energy splitting of related levels (e.g., the σ and σ^* combinations arising from the d_{z^2} levels) is moderate.

From the initial studies of aggregation of d^8 square planar ions in solution, it was suggested that a source of the driving force for aggregation would be donor–acceptor bonding between a filled d_{z^2} orbital on one component with an empty p_z orbital on its partner [39], as shown schematically in Fig. 7.

An excellent analysis of the role of this interaction is found in the work of Aullón and Alvarez [40]. They find p_z—d_{z^2} bonding makes a major contribution to Pt(II)–Pt(II) or Rh(I)–Rh(I) bonding. They also found that π-acidic/acceptor ligands, such as CO, enhance the metal–metal bonding interaction, but π-basic/donor ligands, such as Cl, weaken it. In our complex the π-acidic CO's likely dominate, so that a relatively strong metal–metal bonding interaction can be expected. Balch and coworkers specifically discuss the symmetry-conditioned interplay of p_z—d_{z^2} bonding in dimeric and trimeric $[Rh(alkylisocyanide)_4]^+$ [32].

We also found support for the p_z—d_{z^2} interaction in a natural bond orbital (NBO) 2nd order perturbation theory analysis [41]. A substantial contribution ($E(2) = -75$ kcal/mol) is obtained for just this interaction. The NBO perturbation theory numbers are not to be taken as dimerization energies, as they do not include a large repulsive term. But they are indicative.

We will return to another way to probe this bonding for the polymer.

2.3. An Ir(II)–Ir(II) bonded dimer for comparison

As we mentioned, several Ir(II)–Ir(II) dimers have been synthesized, none of $Ir(CO)_3Cl$ as such. All we know are capped axially by two additional ligands. Fig. 8 shows a simple example, $Cl–Ir(CO)_3Cl–Ir(CO)_3Cl–Cl$. The structural comparison to be made is with the uncapped $Ir(CO)_3Cl$ dimer of Fig. 5. There is some change in the relative rotation of the $Ir(CO)_3Cl$ units, but the major difference is in the Ir–Ir distance, which decreases from 3.05 Å in the weakly associated d^8–d^8 dimer, to 2.79 Å in the Ir–Ir bonded d^7–d^7 dimer. The calculated Ir–Ir bond is a little longer than that observed in the known d^7–d^7 dimers [23,24], but the ligand sets are different in these from our model.

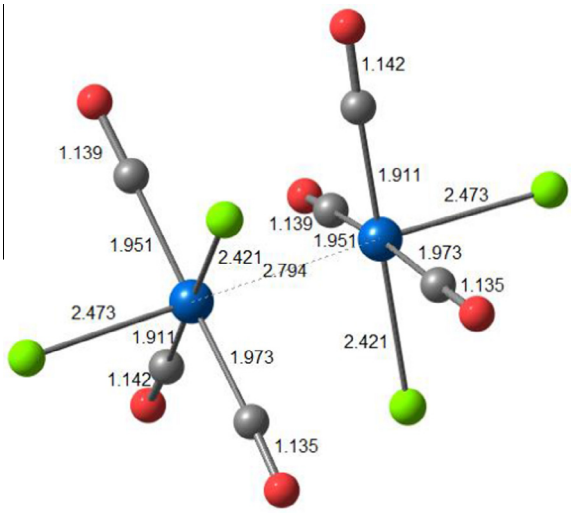

Fig. 8. Calculated geometry of an Ir(II)–Ir(II) dimer.

There is still another measure to distinguish the d^8–d^8 from the d^7–d^7 dimer. The association energy of the former is 15 kcal/mol, that of the latter 47 kcal/mol, both computed from optimized monomer and dimer geometries.

We also did some calculations on Ir(II) dimers with axial ligands X other than chloride (details in SI), in an attempt to emulate the known compounds [23,24]. The Ir–Ir separation is quite variable, ranging between 2.92 Å for X = H, to 2.77 Å for $X = O_3SCF_3$. For another Ir(II)–Ir(II) dimer $(H_3N)Ir(CO)_2Cl_2–Ir(CO)_2Cl_2(NH_3)$, the distance is calculated as 2.73 Å.

2.4. One-dimensional polymers

We next studied with VASP one-dimensional polymers, both "eclipsed" (one molecule per unit cell), and "staggered" (two molecules per unit cell, allowed to seek an optimum dihedral angle Cl–Ir–Ir–Cl). The staggered polymer is more stable, by 0.47 eV (11 kcal/mol) per $Ir(CO)_3Cl$. Its schematic structure is shown in Fig. 9, along with the geometry of the unit cell.

Note that now the optimum Ir–Ir distance is comparable to that observed in the polymer, and this without any further oxidation (beyond Ir(I)).

2.5. Polymer electronic structure

The band structure and density of states (DOS) of the staggered polymer is shown in Fig. 10.

Note the greater than 1 eV band gap for the material. With the functional we use, band gaps are usually underestimated. Thus, there is no indication that such one-dimensional $Ir(CO)_3Cl$ chains, matching well those found in the crystal structure of Reis and Peterson, are metallic.

An extended Hückel calculation on the infinite chain in the VASP-optimized structure (see SI) gives a similar band structure, but a smaller band gap of 0.13 eV. The band structure and gap are in general agreement with a previous extended Hückel calculation [30].

2.6. Approaching the full crystal structure

We did not relish a calculation on the full $Ir(CO)_3Cl$ structure, one view of which is shown in Fig. 1, since $Z = 8$ [6,7]. However, we explored model packings of chains with $Z = 2$ and 4.

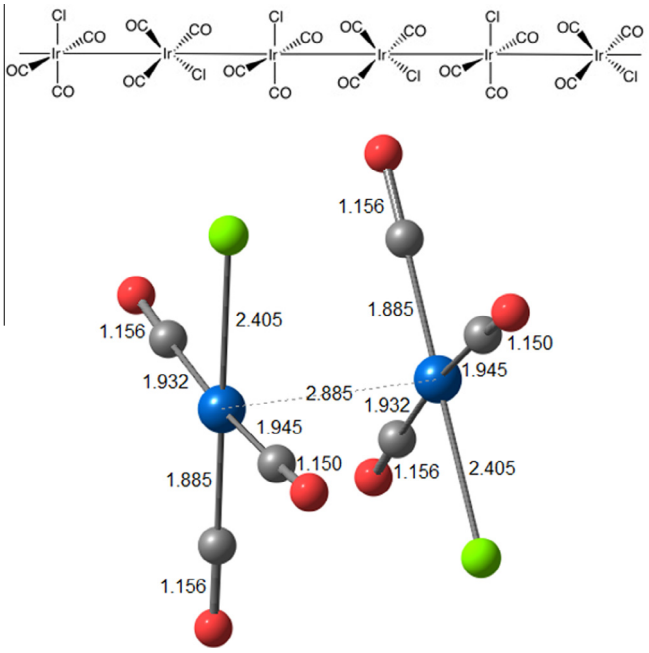

Fig. 9. (top) Schematic drawing of one-dimensional polymer of $Ir(CO)_3Cl$. (bottom) The optimized geometry of a dimeric unit cell of an infinite linear chain of $Ir(CO)_3Cl$.

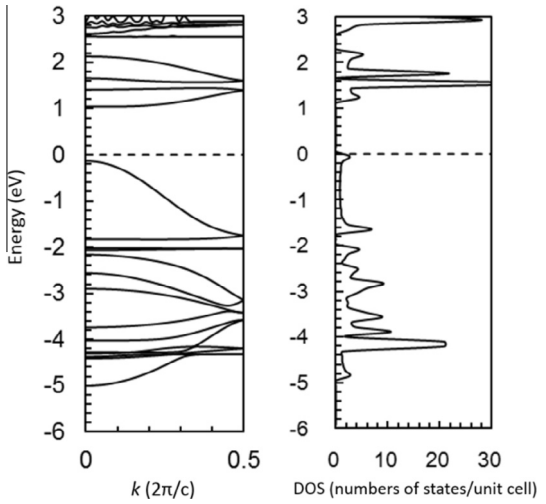

Fig. 10. Band structure, Fermi energy (---), and density of states of a one-dimensional $Ir(CO)_3Cl$ chain.

In the crystal structure studied, the distances between the one-dimensional Ir chains are 6.91, 7.55, and 8.22 Å. We began with a $Z = 2$ structure of tetragonally packed $Ir(CO)_3Cl$. The structure optimized to the structure shown in Fig. 11. Note the chain-to-chain spacing of 7.04 Å is near the smallest chain spacing (6.91 Å) in the observed structure. The Ir–Ir distances in a chain differ in only the third decimal place from those optimized for a model chain "in vacuo" shown in Fig. 9. Though we include a correction for dispersion forces in the calculations, there is no guarantee that it is very accurate. The dispersion correction in the VASP DFT functional plays a role, diminishing the Ir–Ir separation by 0.05 Å to that shown in Fig. 11. Anyway, there is no sign in the distances of anything but weak dispersion forces operating between Ir chains.

The band structure of the $Z = 2$ model would not be expected to differ much from that of the model one-dimensional chain. And Fig. 12 confirms this – note the flat development of the bands along

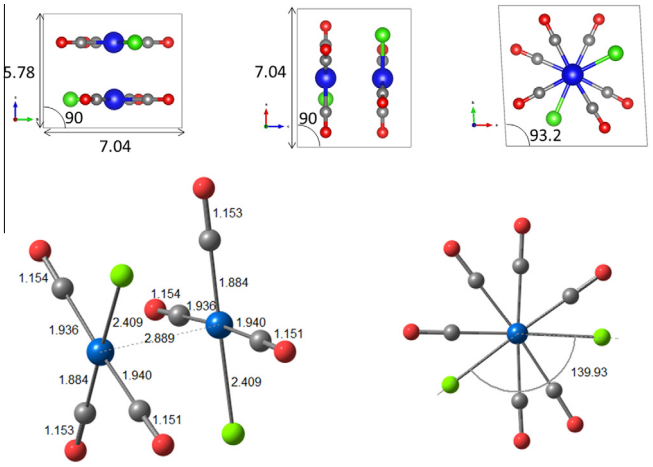

Fig. 11. Optimized $Z = 2$ model for the full crystal structure of $Ir(CO)_3Cl$.

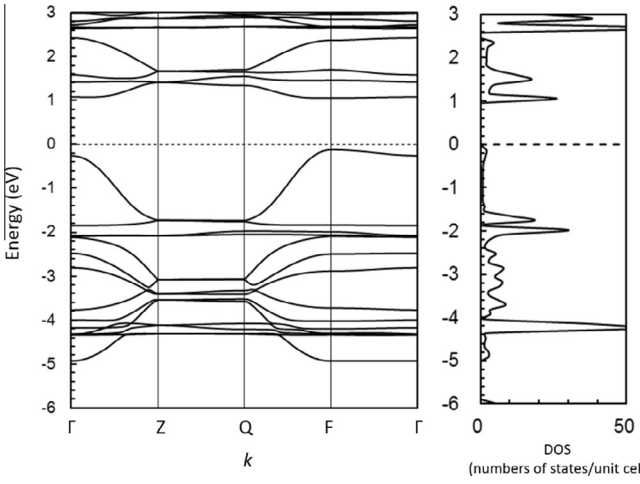

Fig. 12. Band structure, Fermi energy (---), and DOS for $Z = 2$ model of $Ir(CO)_3Cl$.

Γ–F and Z–Q; these are paths along the reciprocal space direction related to unit cell vectors **a** (or **b**). The only significant dispersions are along c, and these may be seen as virtually identical to those of Fig. 10.

We next doubled the unit cell along **a**, and allowed it to reoptimize. This $Z = 4$ model for the full structure (not shown here) gives results nearly identical to those of the $Z = 2$ model discussed above.

We also studied extended structures with other halogen atoms, two monomers per unit cell ($Z = 2$), for $Ir(CO)_3X$, X = F, Cl, Br, I. The Ir–Ir separation goes along this series from 2.83 (F), 2.89 (Cl), 2.91 (Br), to 2.93 (I). We see a modest increase with decreasing electronegativity of the halogen; the result is consistent with some partial oxidation (in the σ-system) of the Ir. A referee has suggested an alternative explanation of this trend, based on increased steric strain. The band gap is independent of the halogen atoms.

2.7. Attempts to oxidize the chain

We first tried to oxidize the $Ir(CO)_3Cl$ chains directly. The highest occupied band in the one-dimensional stack, the one running between 0 and −1.8 eV in Fig. 10, one might think is made up of d_{z^2}—d_{z^2} antibonding levels. But, as we will soon see, this is not so. The top of the valence band is actually slightly Ir–Ir bonding. Thus, removing electrons from this band should not shorten the Ir–Ir separation. We tried to simulate this using a partial charge feature of the VASP programs, and the effect, as Fig. 13 shows,

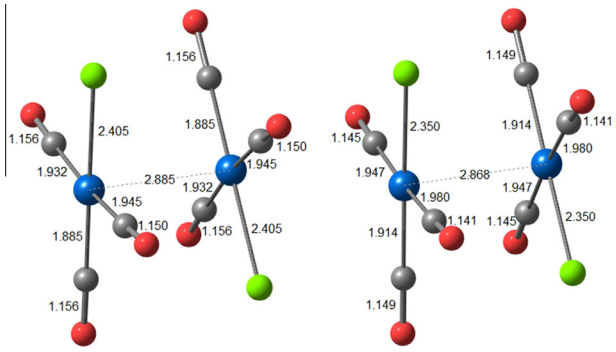

Fig. 13. Geometry of dimer unit in polymer one-dimensional model. At left for neutral polymer, at right for polymer oxidized by 0.5 e per Ir.

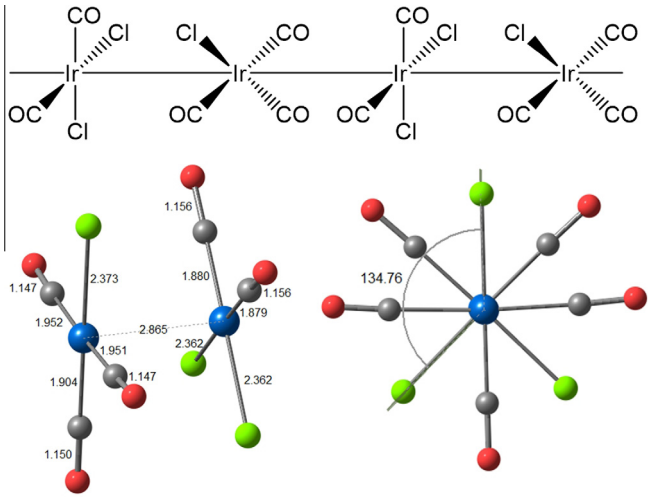

Fig. 14. Optimized geometry of a copolymer of $Ir(CO)_3Cl$ and $Ir(CO)_2Cl_2$.

was reasonably small −a + 1 charge per two $Ir(CO)_3Cl$ units led to a diminution of the Ir–Ir separation by only 0.02 Å. However, experimentally, the effect of oxidation is larger, as described above. The assumption in the theoretical study is of a charge delocalized mixed valence chain.

As expected, the Fermi level of the partially oxidized stack came in the middle of the highest band; such a material should be metallic.

We next tried to examine the effect of introducing some $Ir(CO)_2Cl_2$ into the crystal, effectively partial oxidation of the chain. Only a 1:1 "copolymer" was studied, shown in Fig. 14, along with the optimized structure of a unit cell.

The average oxidation state is now 1.5, and examination of the band structure confirms that the top part of the d_{z^2} band is now emptied. And the stack should now be metallic. Note again that there is only a small decrease in the Ir–Ir separation on oxidation.

2.8. Energetics of polymerization and an essential avoided crossing

This could only be approached with the VASP calculation. Aggregation of monomers into a polymer is computed as quite exothermic, −17 kcal/mol per monomer.

To get some insight into the reasons for aggregations, we turned to an analysis of the projected Crystal Orbital Hamilton Population (pCOHP) of Dronskowski and Blöchl [42]. A negative value of the COHP indicates bonding, and for the polymer, the region (see Fig. 15) below the highest occupied crystal orbital is indeed bonding.

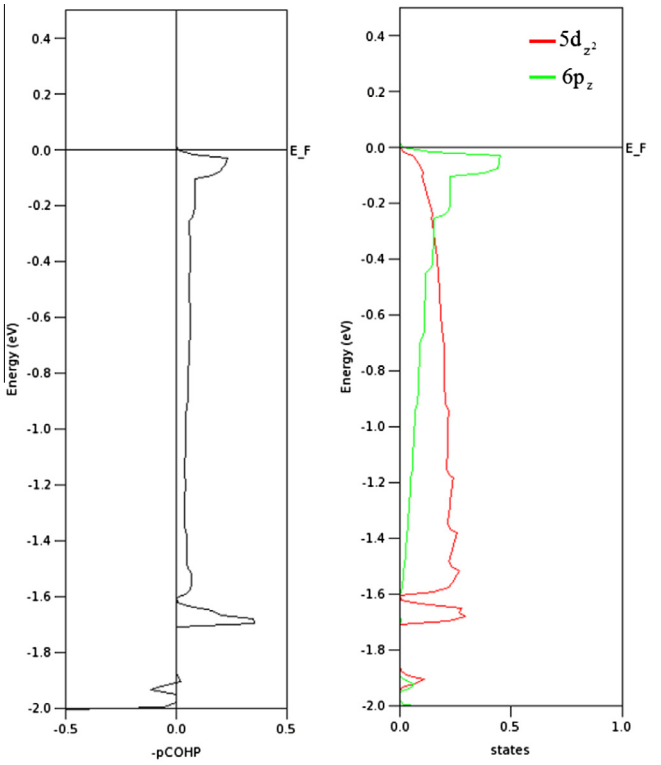

Fig. 15. Negative projected Crystal Orbital Hamilton Population (−pCOHP) for the neighboring Ir–Ir interaction (left) and the contribution of $5d_{z^2}$ and $6p_z$ orbitals of Ir to the DOS (right).

But the top of the valence band in these polymers "should be" made up of σ-antibonding d_{z^2}—d_{z^2} combinations [43,44]. What is going on?

A first clue comes from the decomposition of DOS in this region (right hand side of Fig. 15). It shows much $6p_z$ character at the top of this band. Clearly there must be a lot of $6p_z$—$5d_{z^2}$ mixing in this important energy region. And from our and Aullón and Alvarez analysis of dimer bonding [40], we should have expected this.

We have here a situation of an avoided crossing of bands formed from metal p_z and d_{z^2} levels. This was explicitly seen in the early calculation of Whangbo and Hoffmann [43] for a Pt(II) chain. We probed it in detail here in a series of calculations in which we chose a model $Z = 2$ $Ir(CO)_3Cl$ one-dimensional polymer, and varied the Ir–Ir separation between 2.6 and 3.8 Å. The results, in a way an animation of bonding changes with Ir–Ir separation, are shown in Fig. 16.

As the Ir–Ir distance decreases, one can clearly see the widths of the highest occupied (d_{z^2}) and the lowest unoccupied (p_z) bands expand, leading to a small band gap. When the Ir–Ir distance reaches a certain point in the range from 3.2 to 3.4 Å, a further decrease in the Ir–Ir distance results in a wider band gap. As shown by the PDOS curves, as the Ir–Ir distance decreases, the d_{z^2} character in the highest occupied band decreases and the p_z character increases. The converse occurs in the lowest unoccupied band.

We clearly have an avoided crossing, and as a consequence, as the Ir–Ir distance decreases, an interchange of the d_{z^2} and p_z character occurs. As shown by the −pCOHP curves for the Ir–Ir interaction, as the Ir–Ir distance decreases, the antibonding character due to the out-of-phase combination of the d_{z^2} orbitals decreases below the Fermi level and increases above the Fermi level.

The substantial band gap observed for the optimized structure with the Ir–Ir distance of 2.89 Å is thus due to an avoided crossing, a strong inter-band interaction. As predicted from Fig. 16, if the

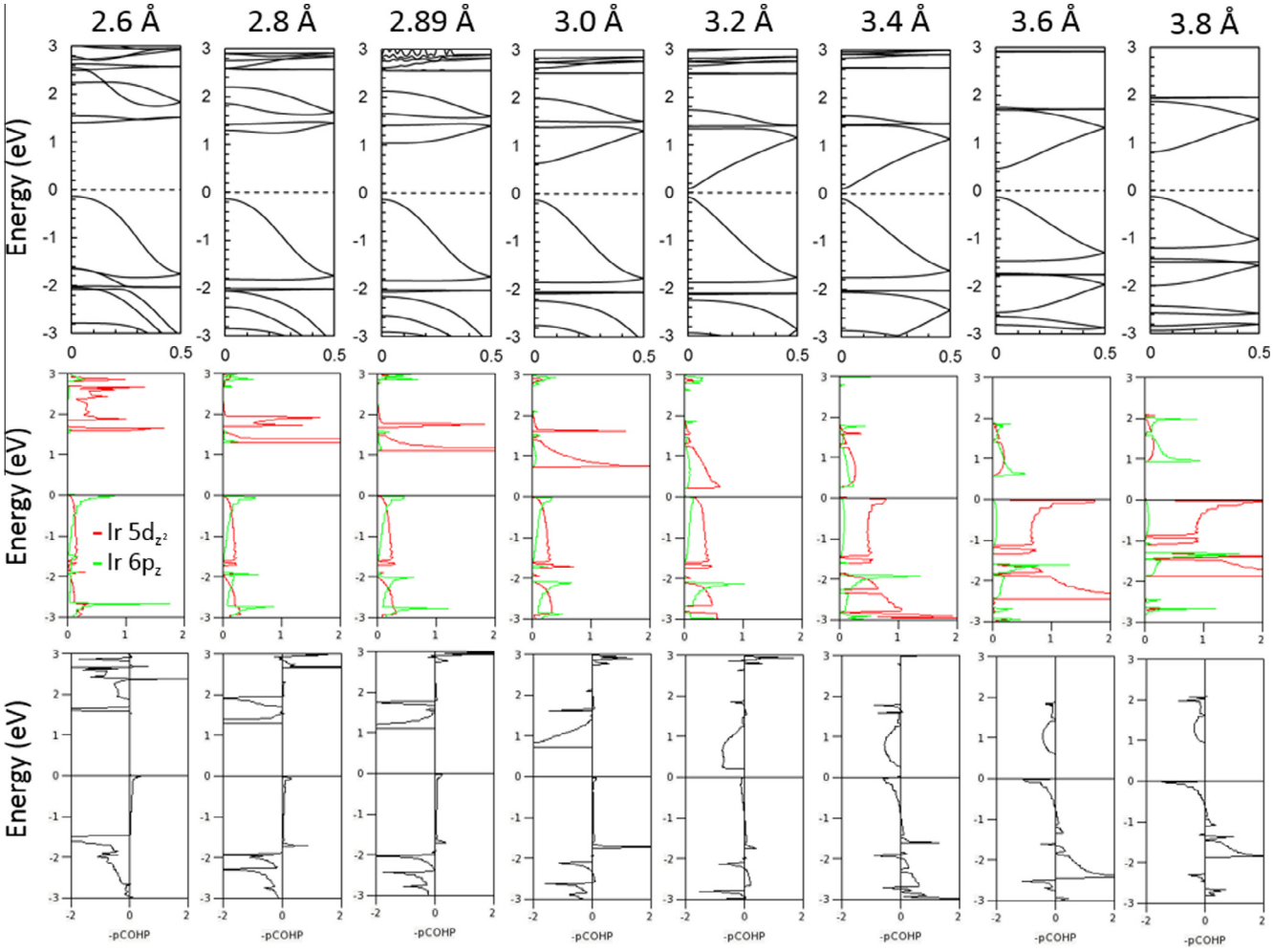

Fig. 16. Band structures (top), contributions from $5d_{z^2}$ (indicated by red) and $6p_z$ (indicated by green) orbitals to DOS (middle), and –pCOHP curves for the neighboring Ir–Ir interaction (bottom) for the one-dimensional $Z = 2$ structures with different Ir–Ir distances in the range from 2.6 to 3.8 Å. (Color online.)

Ir–Ir distance were to fall in the range from 3.2 to 3.4 Å, the Ir chain would have a very small band gap and would be semi-metallic. But then it would likely be unstable both because of the small band gap (an incentive for a 2nd order Jahn–Teller (=Peierls) distortions) and the d_{z^2}—d_{z^2} antibonding near the top of the valence band. We have not studied the distortions that might ensue.

Note that the structure with the Ir–Ir distance of around 3.4 Å would actually have a larger band gap than that shown in Fig. 16 since the DFT method underestimates the band gap. Therefore, the smallest band gap and level crossing would be achieved in a structure with the Ir–Ir distance that is shorter than 3.4 Å. This would result in a smaller band gap in the optimized structure than that shown in Fig. 10. This is just what happens in an extended Hückel calculation (see SI, Fig. S5).

3. Summary comment

Our calculation on stoichiometric isolated dimers, infinite chains, and on a model for the full three-dimensional structure of $Ir(CO)_3Cl$ lead from a computed distance of 3.05 Å in a gas-phase dimer, bound by 15 kcal/mol relative to two monomers, to a staggered chain structure with an Ir–Ir separation of 2.89 Å. That theoretical distance is only 0.05 Å longer than the distance obtained in a crystallographic investigation. And it is reached without any oxidation of the polymer, whether formal or by inclusion of Ir(II) units such as $Ir(CO)_2Cl_2$. In our models for the 3D structure of $Ir(CO)_3Cl$ the band gap remains slightly greater than 1 eV, but we know the methodology underestimates that gap. We describe in detail an avoided crossing in polymer formation, one already incipient in the dimer, and responsible for stabilization of both.

The structure of $Ir(CO)_3Cl$, especially its relatively short Ir–Ir separation, is reproduced by theory. But its weak metallic character remains a mystery, and seems only explainable by partial oxidation.

4. Theoretical methods

All molecular DFT calculations were done by using the GAUSSIAN 09 software [45], with the B3LYP functional [46]. SDD [47] and 6-31G(d) basis sets [48] were chosen for Ir and the other atoms, respectively. To properly account for dispersion interactions, Grimme's D3 dispersion correction with the Becke and Johnson damping function has been added [49]. For calculation of the dimerization energy the counterpoise correction method within the GAUSSIAN 09 package was applied.

All DFT calculations for the extended systems were done by using the Vienna Ab Inito Simulation Package (VASP 5.2.11) [50]. The Kohn–Sham equations were solved with a plane wave basis set using the projector-augmented-wave (PAW) method [51]. The plane-wave energy cutoff was set to be 600 eV. The generalized gradient approximation (GGA) with the Perdew–Burke–Ernzerhof

Table 1
Extended Hückel parameters.

Orbital	H_{ii}(eV)	ζ_1	(c_1)	ζ_2	(c_2)
Ir 6s	−11.36	2.5			
Ir 6p	−4.5	2.2			
Ir 5d	−12.17	5.796	(0.6351)	2.557	(0.5556)
C 2s	−21.4	1.625			
C 2p	−11.4	1.625			
Cl 3s	−26.3	2.183			
Cl 3p	−14.2	1.733			
O 2s	−32.3	2.275			
O 2p	−14.8	2.275			

(PBE) exchange–correlation functional was adopted [52]. The convergence criteria were set to 5×10^{-7} eV for the SCF and 0.005 eV/Å for the geometry optimization. To account for dispersion interactions, Grimme's D2 dispersion correction has been added [53]. All parameters for C, Cl, and O are taken from the Grimme's original paper, but those for Ir are missing [53]. C_6 and R_0 parameters for Ir are set to be 12.54 J nm^6 mol^{-1} and 1.848 Å, respectively [54].

In the optimization of the Ir–Ir distance in the one-dimensional chains with VASP, **a** and **b** axes, which are perpendicular to the chain, were fixed to 15 Å to avoid the inter-chain interactions. The length of **c** axis was changed gradually step by step. In the geometry optimizations the Brillouin zone was sampled by Monkhorst–Pack [55] k-point sets of $2 \times 2 \times 16$ for the $Z = 1$ structure and $2 \times 2 \times 8$ for the $Z = 2$ structure. In the DOS calculations, k-point sets of $2 \times 2 \times 40$ for $Z = 1$ structure and k-point sets of $2 \times 2 \times 20$ for $Z = 2$ structure were used. For the band calculations, 30 k points were sampled along each high symmetry line.

For the full crystal structure calculations, the atomic positions and the cell volume are relaxed. k-Point sets of $4 \times 4 \times 5$ for the $Z = 2$ structure and k-point sets of $2 \times 4 \times 5$ for the $Z = 4$ structure were used. pCOHP curves and atom- and orbital-projected DOS curves are generated with LOBSTER 1.2.0 [42] and visualized in wxDragon 1.9.3 [56]. The pbeVASPFit2015 basis set implemented in LOBSTER was used. The charge spilling values are always lower than 0.65%, which suggests that LOBSTER be able to transfer more than 99% of the charge density from the VASP-generated plane waves into the local orbitals.

Extended Hückel calculations were carried out with the YAeHMOP program [57]. The VASP-optimized structures were used. Parameters used for Ir, C, Cl, and O appear in Table 1. A 50-k point set was used.

Acknowledgments

Y.T. thanks the Japan Society for the Promotion of Science for a JSPS Postdoctoral Fellowship for Research Abroad. Our work at Cornell was supported by the National Science Foundation through Grant CHE-1305872.

Appendix A. Supplementary data

Supplementary data associated with this article can be found, in the online version, at http://dx.doi.org/10.1016/j.poly.2015.09.050.

References

[1] (a) W. Hieber, H. Lagally, Z. Anorg. Allgem. Chem. 245 (1940) 321;
(b) W. Hieber, H. Lagally, H. Mayr, Z. Anorg. Allgem. Chem. 246 (1941) 138.
[2] E.O. Fisher, K.S. Brenner, Z. Naturforsch. 17b (1962) 774.
[3] (a) L. Malatesta, M. Angoletta, J. Inorg. Nucl. Chem. 8 (1958) 275;
(b) L. Malatesta, F. Canjiani, J. Inorg. Nucl. Chem. 19 (1961) 81.
[4] K.W. Krogman, W. Binder, H.D. Hausen, Angew. Chem., Int. Ed. Engl. 7 (1968) 812.
[5] A.P. Ginsberg, R.L. Cohen, F.J. DiSalvo, K.W. West, J. Chem. Phys. 60 (1974) 2657.
[6] A.H. Reis, S.W. Peterson, Structure and oxidation states of Ir and Pt. One-dimensional inorganic complexes, Ann. N.Y. Acad. Sci. 313 (1978) 560.
[7] A.H. Reis Jr., V.S. Hagley, S.W. Peterson, J. Am. Chem. Soc. 99 (1977) 4184.
[8] A.H. Reis, in: J.S. Miller (Ed.), Extended linear chain compounds, Vol. 1, Plenum, New York, 1982, pp. 157–196.
[9] J.M. Williams, A.J. Schulz, A.E. Underhill, K. Carneiro, in: J.S. Miller (Ed.), Extended Linear Chain Compounds, Vol. 1, Plenum, New York, 1982, pp. 73–156.
[10] N.A. Bailley, E. Coates, G.B. Robertson, F. Bonati, R. Ugo, Chem. Commun. (1967) 1041.
[11] E.M. Gussenhoven, M.M. Olmstead, J.C. Fettinger, A.L. Balch, Inorg. Chem. 47 (2008) 4570.
[12] H. Huang, N.R. Hurubeanu, C.J. Bourgeois, S. Cheah, J. Yuan, A.L. Rheingold, R.P. Highes, Can. J. Chem. 87 (2009) 151.
[13] S.M. Trzaska, T.M. Swager, Chem. Mater. 10 (1998) 438.
[14] K.V. Zherikova, N.V. Kuratieva, N.B. Morozova, J. Struct. Chem. 50 (2009) 574.
[15] A.P. Ginsberg, J.W. Koepke, J.J. Hauser, K.W. West, F.J. Di Salvo, C.R. Sprinkle, R. L. Cohen, Inorg. Chem. 15 (1976) 514.
[16] K. Winkler, M. Wysocka-Żołopa, M.M. Oleksicka, K. Rećko, L. Dobrzyński, J.R. Stork, E.M. Gussenhoven, M.M. Olmstead, A.L. Balch, Electrochim. Acta 53 (2008) 7288.
[17] M. Wysocka, K. Winkler, J.R. Stork, A.L. Balch, Chem. Mater. 16 (2004) 771.
[18] M.A. Ciriano, D.-C.S. Sebastián, L.A. Oro, A. Tiripicchio, M.T. Camellini, F.J. Lahoz, Angew. Chem., Int. Ed. Engl. 27 (1988) 402.
[19] C. Tejel, M.A. Ciriano, J.A. López, F.J. Lahoz, L.A. Oro, Angew. Chem., Int. Ed. 37 (1998) 1542.
[20] C. Tejel, M.A. Ciriano, B.E. Villarroya, R. Gelpi, J.A. López, F.J. Lahoz, L.A. Oro, Angew. Chem., Int. Ed. 40 (2001) 4084.
[21] C. Tejel, M.A. Ciriano, B.E. Villarroya, J.A. López, F.J. Lahoz, L.A. Oro, Angew. Chem., Int. Ed. 42 (2003) 530.
[22] B.E. Villarroya, C. Tejel, M.M. Rohmer, L.A. Oro, M.A. Ciriano, M. Bénard, Inorg. Chem. 44 (2005) 6536.
[23] S.K. Patra, S.M.W. Rahaman, M. Majumdar, A. Singha, J.K. Bera, Chem. Commun. (2008) 2511.
[24] H. Huang, A.L. Rheingold, R.P. Hughes, Organometal 28 (2009) 1575.
[25] H.-C. Böttcher, P. Mayer, Z. Anorg. Allg. Chem. 639 (2013) 234.
[26] D.E. Bikiel, J.M. Ramallo-López, F.G. Requejo, O.B. Oña, M.B. Ferraro, J.C. Facelli, F. Doctorovich, Polyhedron 30 (2011) 221.
[27] J.S. Miller, A.J. Epstein, Progr. Inorg. Chem. 20 (1976) 1.
[28] F.L. Lecrone, M.J. Minot, J.H. Perlstein, Inorg. Nucl. Chem. Lett. 8 (1972) 173.
[29] J.W. McKenzie, C.-H. Wu, R.H. Bube, Appl. Phys. Lett. 21 (1972) 187.
[30] D. Bhaumik, J.E. Mark, Synth. Met. 6 (1983) 299.
[31] See Ref. 23 in Ref. 8.
[32] N.T. Tran, J.R. Stork, D. Pham, M.M. Olmstead, J.C. Fettinger, A.L. Balch, Chem. Comm. (2006) 1130.
[33] See references in A.L. Balch, in: J.S. Miller, (Ed.), Extended linear chain compounds, Vol. 1, 1982, Plenum, New York, 1982, pp. 157–196. See also K.R. Mann, H.B. Gray, Adv. Chem. Ser. 173 (1979) 225, and S.F. Rice, S.J. Milder, H.B. Gray, R.A. Goldbeck, D.S. Kliger, Coord. Chem. Rev. 43 (1982) 349.
[34] G.M. Finniss, E. Canadell, C. Campana, K.R. Dunbar, Angew. Chem., Int. Ed. Engl. 35 (1996) 2772.
[35] (a) J.J. Novoa, G. Aullón, P. Alemany, S. Alvarez, J. Am. Chem. Soc. 117 (1995) 7169;
(b) S. Alvarez, G. Aullón, R. Fandos, J.L.G. Fierro, P. Ocón, A. Otero, S. Rojas, P. Terreros, Dalton Trans. (2005) 938.
[36] X. Zhou, H.-X. Zhang, Q.-J. Pan, M.-M. Li, Y. Wang, C.-M. Che, Eur. J. Inorg. Chem. (2007) 2181.
[37] B.-H. Xia, C.-M. Che, Z.-Y. Zhou, Chem. Eur. J. 9 (2003) 3055.
[38] A. Poater, S. Moradell, E. Pinilla, J. Poater, M. Solà, M.Á. Martínez, A. Llobet, Dalton Trans. (2006) 1188.
[39] K.R. Mann, J.G. Gordon II, H.B. Gray, J. Am. Chem. Soc. 97 (1975) 3553.
[40] G. Aullón, S. Alvarez, Chem. Eur. J. 3 (1997) 655.
[41] A.E. Reed, L.A. Curtiss, F. Weinhold, Chem. Rev. 88 (1988) 899.
[42] (a) R. Dronskowski, P.E. Blöchl, J. Phys. Chem. 97 (1993) 8617;
(b) V.L. Deringer, A.L. Tchougreeff, R. Dronskowski, J. Phys. Chem. A 115 (2011) 5461;
(c) S. Maintz, V.L. Deringer, A.L. Tchougreeff, R. Dronskowski, J. Comput. Chem. 34 (2013) 2557.
[43] M.-H. Whangbo, R. Hoffmann, J. Am. Chem. Soc. 100 (1978) 6093.
[44] R. Hoffmann, Solid and Surfaces, A Chemist's View of Bonding in Extended Structures, Wiley, New York, 1988.
[45] M.J. Frisch, G.W. Trucks, H.B. Schlegel, G.E. Scuseria, M.A. Robb, J.R. Cheeseman, G. Scalmani, V. Barone, B. Mennucci, G.A. Petersson, Gaussian 09, Revision D.01, Gaussian Inc, Wallingford CT, 2009.
[46] (a) A.J. Becke, Chem. Phys. 98 (1993) 5648;
(b) C. Lee, W. Yang, R. Parr, Phys. Rev. B 37 (1988) 785;
(c) S. Vosko, L. Wilk, M. Nusair, Can. J. Phys. 58 (1980) 1200.
[47] D. Andrae, U. Haeussermann, M. Dolg, H. Stoll, H. Preuss, Theor. Chim. Acta 77 (1990) 123.
[48] R. Krishnan, J.S. Binkley, R. Seeger, J.A. Pople, J. Chem. Phys. 72 (1980) 650.
[49] (a) S. Grimme, J. Antony, S. Ehrlich, H. Krieg, J. Chem. Phys. 132 (2010) 154104;
(b) S. Grimme, S. Ehrlich, L. Goerigk, J. Comput. Chem. 32 (2011) 1456;
(c) A.D. Becke, E.R. Johnson, J. Chem. Phys. 122 (2005) 154104;

(d) E.R. Johnson, A.D. Becke, J. Chem. Phys. 123 (2005) 024101;
(e) A.D. Becke, E.R. Johnson, J. Chem. Phys. 124 (2006) 014104.
[50] (a) G. Kresse, J. Hafner, Phys. Rev. B 47 (1993) 558;
(b) G. Kresse, J. Hafner, Phys. Rev. B 49 (1994) 14251;
(c) G. Kresse, J. Furthmüller, Comput. Mat. Sci. 6 (1996) 15;
(d) G. Kresse, J. Furthmüller, Phys. Rev. B 54 (1996) 11169.
[51] (a) P.E. Blochl, Phys. Rev. B 50 (1994) 17953;
(b) G. Kresse, D. Joubert, Phys. Rev. B 59 (1999) 1758.
[52] (a) J.P. Perdew, K. Burke, M. Ernzerhof, Phys. Rev. Lett. 77 (1996) 3865;
(b) J.P. Perdew, K. Burke, M. Ernzerhof, Phys. Rev. Lett. 78 (1997) 1396.
[53] S. Grimme, J. Comp. Chem. 27 (2006) 1787.
[54] These values are the same as those implemented in the Atomistix Tool Kit (ATK v. 2014.2, Quantum Wise A/S (quantumwise.com)). According to a customer officer of Quantum Wise, they obtained these values by communicating directly with the author of a paper, Phys. Rev. Lett. 107 (2011) 36101.
[55] H.J. Monkhorst, J.D. Pack, Phys. Rev. B 13 (1976) 5188.
[56] B. Eck, wxDragon, Aachen, Germany, 1994–2013; available at http://www.wxdragon.de.
[57] G.A. Landrum, YAeHMOP: Yet Another extended Hückel Molecular Orbital Package, Version 3.0; http://sourceforge.net/projects/yaehmop/.